Microfluid Nanofluid
DOI 10.1007/s10404-010-0616-1

SHORT COMMUNICATION

Continuous separation of non-magnetic particles inside ferrofluids

Taotao Zhu · Francisco Marrero · Leidong Mao

Received: 6 February 2010 / Accepted: 5 April 2010

Abstract We present a novel and label-free continuous flow non-magnetic microparticle separation scheme in a microfluidic device under static magnetic fields. The separation process is conducted inside water-based ferrofluids. We exploit the difference in particle sizes to achieve binary separation of microparticles with high throughput. We demonstrate size-based separation (1 and 9.9 μm, 1.9 and 9.9 μm, 3.1 and 9.9 μm) of microparticles with a minimum of 10^5 particles/h throughput and close to 100% separation efficiency.

Keywords Particle separation · Ferrofluid · Magnetic buoyancy force

1 Introduction

Microfluidic devices for microparticle and cellular separation are becoming increasingly important in miniaturized biological applications (Nolan and Sklar 1998; Toner and Irimia 2005; Yung et al. 2009). Existing separation methods, including techniques based on channel geometry (Takagi et al. 2005; Yamada and Seki 2005) and obstacle design (Huang et al. 2004), optical force (MacDonald et al. 2003), dielectrophoresis (Voldman 2006), and magnetic bead labeling (Yung et al. 2009), have their own shortcomings. Techniques based on geometries use appropriate channel and obstacle design to direct particles of different sizes into separate flow streamlines. The dimensions of the channels and obstacles have implications for the applicable separation size range, and a significant amount of fine-tuning is often necessary for the separation of small particles. The optical tweezer technique employs the forces exerted by a focused laser beam to manipulate nano- to micro-scale objects. This method is usually applied to move and trap a single object. The heating due to the focused laser beam can potentially damage living systems. Dielectrophoresis has the potential to realize integrated devices for high-throughput manipulation of microparticles or cells. However, its performance usually depends on the electrical properties of the specific liquid medium, particle shape, and its effective dielectric constant. The alternating electric fields may polarize the cell membranes and lead to cell death. The magnetic bead labeling technique, on the other hand, uses functionalized magnetic beads to label and separate target particles and cells. This approach takes long incubation time and is manually intensive. There is also the difficulty of removing the magnetic labels from the target particles or cells prior to further analysis.

In an attempt to address some of the aforementioned limitations, we have developed a novel microfluidic device that can continuously separate non-magnetic microparticles based on their sizes inside water-based ferrofluids with the use of a simple permanent magnet. Our approach uses the ferrofluid as a uniform magnetic environment that surrounds the non-magnetic particles within the microfluidic channel. Ferrofluids are colloidal mixtures of magnetic nanoparticles (Rosensweig 1985). The nanoparticles are usually covered by a surfactant, and suspended in a compatible liquid medium. Ferrofluid hydrodynamics (ferrohydrodynamics) have been extensively studied both theoretically (Mao and Koser 2005; Rinaldi and Zahn

T. Zhu · F. Marrero
Department of Chemistry, Nanoscale Science and Engineering Center, The University of Georgia, Athens, GA 30602, USA

L. Mao (✉)
Faculty of Engineering, Nanoscale Science and Engineering Center, The University of Georgia, Athens, GA 30602, USA
e-mail: mao@uga.edu

Published online: 20 April 2010

2002; Zahn and Greer 1995) and experimentally (Mao and Koser 2006) in the past. Non-magnetic microparticles inside ferrofluids experience a magnetic buoyancy force under non-uniform magnetic fields (Rosensweig 1966). This phenomenon has been used to manipulate particles to form ordered crystalline structure in diluted ferrofluids (Skjeltorp 1983). Ferrofluids have also been used for separating materials by their density. A non-uniform magnetic field was used to create a magnetic pressure distribution in the ferrofluid. The fluid acted as if it had variable density with height. This phenomenon formed the foundation for the magnetohydrostatic separation of ores (Rosensweig 1985; Rosensweig et al. 1987). The same principle was used to separate large particles based on their densities' difference in magnetic $GdCl_3$ solution (Winkleman et al. 2007). Recently, Yellen et al. (2005) demonstrated the transportation and assembly of colloidal particles inside ferrofluids on top of a substrate with microfabricated periodic micromagnets and suggested a particle sorting scheme based on their devices. Kose et al. (2009) experimentally demonstrated an integrated microfluidic platform for the controlled sorting of micron-sized particles under traveling magnetic fields in static flow conditions. They reported size-based separation of 173 particles of 9.9 μm diameter from 1294 particles of 2.2 μm diameter with 99.3% separation efficiency in less than 1 min. Our approach, on the other hand, adopts a continuous flow configuration thus can achieve a higher (e.g., $\sim 10^5$ particles/h) throughput. The device fabrication only needs a simple soft lithography step (Xia and Whitesides 1998) and does not require microfabricated micromagnets or current-carrying electrodes, which significantly increase the cost associated with the device. The operation of the device is straightforward and the resulting separation efficiency of large particles from polydispersed particles mixture is 100%.

2 Working mechanism

A schematic of a prototype microfluidic separation device is shown in Fig. 1a. Non-magnetic microparticles mixed with water-based ferrofluids were introduced into the microfluidic channel and hydrodynamically focused by the ferrofluid sheath flow. Once entering the separation region, deflections of non-magnetic particles from their flow paths occurred because of the magnetic buoyancy forces on them under non-uniform magnetic fields. Particles of larger size experienced more magnetic forces than smaller ones. This is because magnetic buoyancy forces are proportional to the volume of the particles. The hydrodynamic drag force, on the other hand, scales with the diameter of the particles. As a result, larger particles were deflected more than small

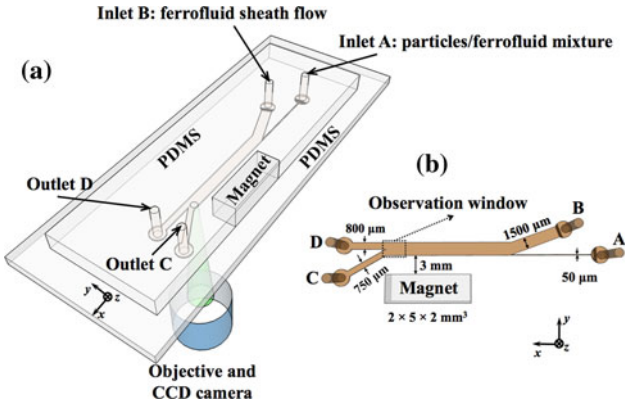

Fig. 1 **a** Schematic representation of the separation mechanism and the experimental setup. Non-magnetic microparticles and ferrofluid mixture were introduced into the microfluidic channel (20 μm in thickness) Inlet *A* and hydrodynamically focused by the ferrofluid sheath flow from Inlet *B*. Upon entering the separation region (near the permanent magnets), deflection of microparticles from their flow paths occurred because of the non-uniform magnetic field produced by permanent magnets. We used a stack of four magnets in our experiments. Here we only drew one for simplicity. The motion of the microparticles was imaged from the observation window through a 5× objective and a CCD camera. Particle samples collected from Outlets *C* and *D* were analyzed for size distribution. **b** The dimensions of the microfluidic channel and the magnets, and the location of the observation window

ones. This phenomenon can be used to continuously separate non-magnetic particles inside ferrofluid based on their sizes.

The dynamics of a non-magnetic microparticle inside a ferrofluid-filled microfluidic channel is determined primarily by the balance of the hydrodynamic viscous drag and the magnetic buoyancy force on that particle. Given the magnitude of the magnetic fields in our experiments, gravitational force and buoyancy force are second order and therefore not important. When the non-magnetic particles are sufficiently small, Brownian motion and diffusion will start to affect the motion of the particles. A criterion developed by Gerber et al. (1983) can be used to estimated the critical diameter, which in our case is on the order of 10 nm, much smaller than the diameters of large particles used in our experiments. Therefore, diffusion effect of large particles inside ferrofluids can be neglected. For small particles (<1 μm diameter) in ferrofluids, diffusion needs to be considered.

When an external magnetic field gradient is applied, the non-magnetic particles inside ferrofluids experience both magnetic and hydrodynamic drag forces, $\mathbf{F}_m$ and $\mathbf{F}_d$. In the cases of diluted ferrofluids or an intense applied magnetic field, the magnetic buoyancy force on a non-magnetic particle inside ferrofluids can be expressed as (Rosensweig 1966)

$$\mathbf{F}_m = -V\mu_0(\mathbf{M}\cdot\nabla)\mathbf{H}$$

where V is the volume of the non-magnetic particle and μ_0 is the permeability of free space. $\mathbf{M}$ is the effective magnetization of the ferrofluid and $\mathbf{H}$ is the applied magnetic field. The presence of the minus sign in front of the term indicates the non-magnetic particle immersed in ferrofluids experiences a force in the direction of the weaker magnetic field. The effective magnetization of ferrofluid $\mathbf{M}$ is related to the magnetization of ferrofluid $\mathbf{M}_f$ through a "demagnetization" factor, which accounts for the shape-dependent demagnetization of the concentrated ferrofluid by the presence of the non-magnetic particle. EMG 408 ferrofluid used in our experiments is very diluted, therefore we assume the "demagnetization" field is small enough so that $\mathbf{M}$ equals to $\mathbf{M}_f$.

We take the hydrodynamic drag on a non-magnetic particle in ferrofluids to be the Stokes drag,

$$\mathbf{F}_d = 3\pi\eta D(\mathbf{v}_f - \mathbf{v}_p)f_D$$

where η is the viscosity of the ferrofluid, D is the diameter of the spherical particle, and $\mathbf{v}_f$ and $\mathbf{v}_p$ are the velocity vectors of the ferrofluid and the particle, respectively. f_D is the hydrodynamic drag force coefficient. Its appearance indicates the increased fluid viscosity the large non-magnetic particle experiences as it moves near the microfluidic channel surface (Ganatos et al. 1980; Krishnan and Leighton 1995; Staben et al. 2003).

$$f_D = \left[1 - 0.6526\left(\frac{D}{D+2z}\right) + 0.1475\left(\frac{D}{D+2z}\right)^3 - 0.131\left(\frac{D}{D+2z}\right)^4 - 0.0644\left(\frac{D}{D+2z}\right)^5\right]^{-1}$$

where z is the distance between the bottom of the particle and the channel surface.

3 Experimental details

We used a commercial water-based magnetite ferrofluid (EMG 408, Ferrotec Co., Bedford, NH) for the separation experiments. The volume fraction of the magnetite particles for this particular ferrofluid is 1.1%. The mean diameter of nanoparticles has been determined from transmission electron microscopy (TEM) images to be 10.2 nm with a standard deviation of 1.25 nm. The initial magnetic susceptibility is 0.26. Different sizes (1, 1.9, 3.1, and 9.9 μm diameters) of green fluorescent polystyrene spherical microparticles (Thermo Fisher Scientific Inc., Waltham, MA) with a density of 1.05 g/cm^3 were used. The coefficient of variation (the ratio of the standard deviation to the mean) of the microparticle diameters was less than 5%. In order to obtain the target particle concentrations ($\sim 10^6$ particles/cm^3) in ferrofluids, the fluorescent particles suspension was first diluted with DI water containing 0.1% Tween 20 to prevent particle aggregation. For 1 and 1.9 μm particles, the initial concentrations were relatively high; the diluted particle suspensions were diluted again with EMG 408 ferrofluids to achieve target concentrations (1 μm, 1.8×10^6 particles/cm^3; 1.9 μm, 2.6×10^6 particles/cm^3). For 3.1 and 9.9 μm particles, the initial concentrations were relatively low; the diluted particle suspensions were centrifuged, decanted then mixed with EMG 408 ferrofluids to achieve target concentrations (3.1 μm, 6.0×10^6 particles/cm^3; 9.9 μm, 1.9×10^6 particles/cm^3).

The PDMS microfluidic channel was fabricated through a standard soft-lithograph approach (Xia and Whitesides 1998) and attached to the flat surface of another piece of PDMS. The dimensions of the microfluidic channel are listed in Fig. 1b. The thickness of the channel was measured to be 20 μm by a profilometer (Dektak 150, Veeco Instruments Inc., Chadds Ford, PA). Treating both PDMS surfaces before attachment with a plasma cleaner (PDC-32G, Harrick Plasma, Ithaca, NY) at 11.2 Pa O_2 partial pressure with 18 W power for 1 min rendered them hydrophilic and made the PDMS attachment permanent. The experiment was conducted on the stage of an inverted microscope (Zeiss Axio Observer, Carl Zeiss Inc., Germany). Before liquid injection, the completed device was exposed again to plasma for 10 min to keep the surfaces hydrophilic. Triton X-100 solution was injected into the channel using a syringe pump (KDS 101, KD Scientific, Holliston, MA). The solution was kept in the channel for 20 min then purged with N_2 gas. This step ensured that the polystyrene particles would not attach to PDMS surfaces during experiment. The microfluidic channel was afterwards filled with air-bubble free EMG 408 ferrofluid. During experiments, ferrofluid injection into Inlet B was maintained at 10 μl/min using a syringe pump (KDS 101, KD Scientific, Holliston, MA). Ferrofluid and particles mixture was injected into Inlet A at 3 μl/min using a second syringe pump (Nexus 3000, Chemyx Inc., Stafford, TX). The ferrofluid and particles mixture stream were focused before entering the separation region. A non-uniform magnetic field was generated by a stack of four NdFeB permanent magnets. Each magnet is 2 mm in width, 5 mm in length, and 2 mm in thickness. The magnets stack was placed 3 mm away from microfluidic channel as indicated in Fig. 1b. The magnetic flux density at the center of the magnets' pole surface was measured to be 0.47 T by a Gauss meter (Model 5080, Sypris, Orlando, FL) and an axial probe with 0.381 mm diameter of circular active area. The images of fluorescent particles were recorded through a fluorescent filter set (41001 FITC, Chroma Technology Corp., Rockingham, VT) and a 5× objective with a CCD camera (SPOT RT3, Diagnostic Instruments, Inc., Sterling Heights, MI). Particle samples

collected from Outlets C and D (see Fig. 1b) were analyzed for size distribution in order to quantitatively evaluate the separation efficiency of this approach. ImageJ® software was used to count the particles.

4 Results and discussion

In the experiment with 1 μm diameter and 9.9 μm diameter fluorescent microparticles, we introduced the microparticles mixture ($\sim 10^6$ particles/cm^3 concentration for both particles) into the microfluidic channel Inlet A at a constant flow rate of 3 μl/min. The mixture was hydrodynamically focused into a very narrow stream by the sheath flows from Inlet B at a constant flow rate of 10 μl/min. Before the non-uniform magnetic field was applied, small particles and large particles were observed to flow together near the sidewall of the channel, as shown in Fig. 2a. Due to the opaqueness of the ferrofluid, the particles were only visible when they were very close to the bottom surface of the channel. Because the thickness of the microfluidic channel was 20 μm, large particles (9.9 μm diameter) became more visible than small particles (1 μm diameter) in fluorescent mode. The particles appeared to be line segments instead of dots because of the CCD camera's exposure time and high flow speed (2.1 mm/s) in the channel. Once the magnetic field was applied, magnetic buoyancy forces deflected the microparticles from their flow paths, as shown in Fig. 2d. The magnetic buoyancy force on large particles was greater than those acting on the small particles, deflecting the large particles out of the particles mixture and toward Outlet D. The magnetic buoyancy forces on small particles were inadequate to deflect them into Outlet D; therefore they exited the channel through Outlet C. This resulted in the spatial separation of these two particles at the end of the separation region. Both small and large particles were visible in fluorescent mode after the magnetic field was applied. This was because the permanent magnets produced a weak but non-zero z-direction magnetic field, which effectively pushed all non-magnetic particles in ferrofluid down to the bottom surface of the microfluidic channel. We were able to separate $\sim 10^5$ 9.9 μm particles from $\sim 10^5$ 1 μm particles/h with the aforementioned flow rates. Figure 2b and e depicts the separation of 1.9 μm diameter and 9.9 μm diameter particles. Figure 2c and f depicts the separation of 3.1 μm diameter and 9.9 μm diameter particles. The separation throughputs were both on the order of 10^5 particles/h. Noted that the separation throughput can be further increased by tuning the experimental parameters (increasing the flow rates of the particles/ferrofluid mixture and magnetic field strength, gradient). Given a range of particle sizes, the resolution of this separation approach is directly related to the difference in the particles' y-direction deflection (see Fig. 1b) towards the Outlets. Ideally, the resolution of separation could be arbitrarily small. However, particle streams have a finite width in the separation region of the channel due to the device design and their small but non-zero diffusions in

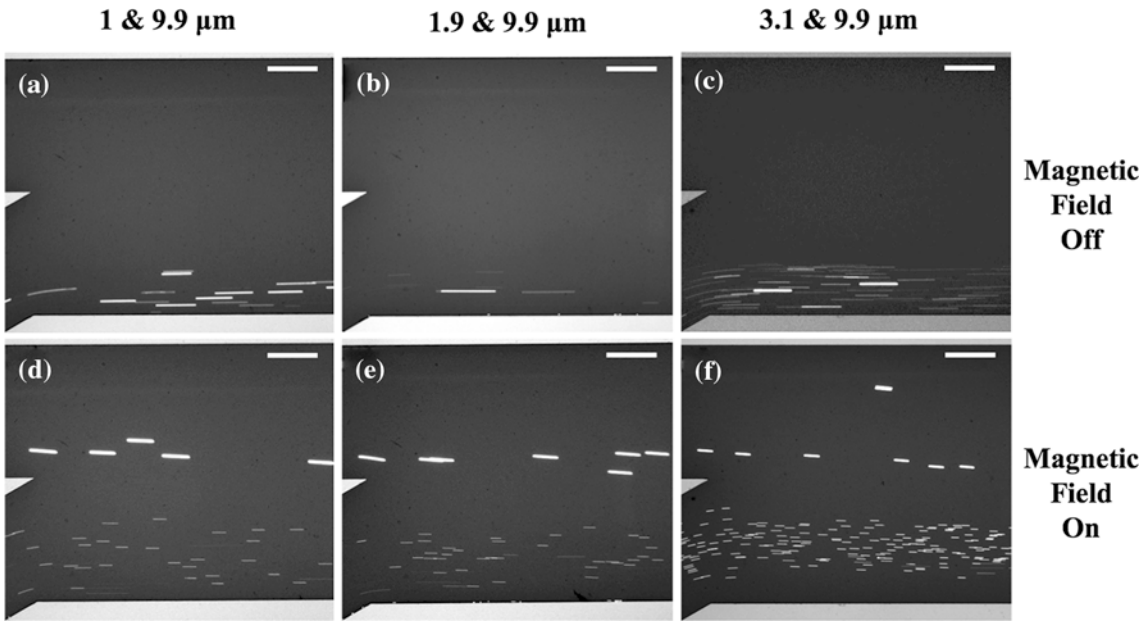

Fig. 2 Experimental top view of the observation window, **a–c** were the recorded fluorescent images of particles mixture motions (**a** 1 and 9.9 μm particles; **b** 1.9 and 9.9 μm particles; **c** 3.1 and 9.9 μm particles) before the magnetic field is applied, **d–f** were the images after the magnetic field was applied. The *scale bars* represent 300 μm

ferrofluids. The difference in the particles' *y*-direction deflections needs to be larger than the width of the small particles' stream in order for the separation approach to be useful. A future work for this study is to optimize the microfluidic channel design such that the width of the particles' stream inside ferrofluids is much smaller compared to the current design. The separation resolution of this approach can be further increased as a result. Non-magnetic particle separation within ferrofluids works as long as particles are much larger than the magnetic nanoparticles and the average spacing between them. Non-magnetic particles with the diameter on the order of 10 nm will tend to get lodged between the magnetite nanoparticles instead of being pushed when an external field is applied. Therefore, the size of target non-magnetic particles for this separation method to work needs to be much larger than 10 nm. Currently, the smallest particles' diameter we can separate using this approach is 1 μm. Non-magnetic particles inside ferrofluid without any flow are prone to chaining and clustering under magnetic fields (Skjeltorp 1983). However, the chaining and clustering effects appeared to be minimal in our separation device, possibly due to the fact the flow speed in our device was high enough so that the shear force was able to prevent the particles aggregate from forming.

To precisely evaluate the separation efficiency of this approach, the separated particle samples were collected from the Outlets C and D and analyzed for size distribution off chip. ImageJ® software was used to count the number of the particles from both outlets. In our experiments, a mixture of particles with different sizes was eventually separated into Outlets C and D. We defined the remaining efficiency as the ratio of the number of the particles (e.g., 1 μm particles) exiting from Outlet C after magnetic field application to their corresponding number before magnetic field application. Similarly, separation efficiency was defined as the ratio of the number of the particles (e.g., 9.9 μm particles) exiting from Outlet D after magnetic field application to their corresponding number before magnetic field application. Figure 3a shows a representative fluorescent image of the polydispersed particles mixture (1 and 9.9 μm) collected from Inlet A before separation. When the focused particles stream was introduced into the separation region of our device, virtually all small particles remained

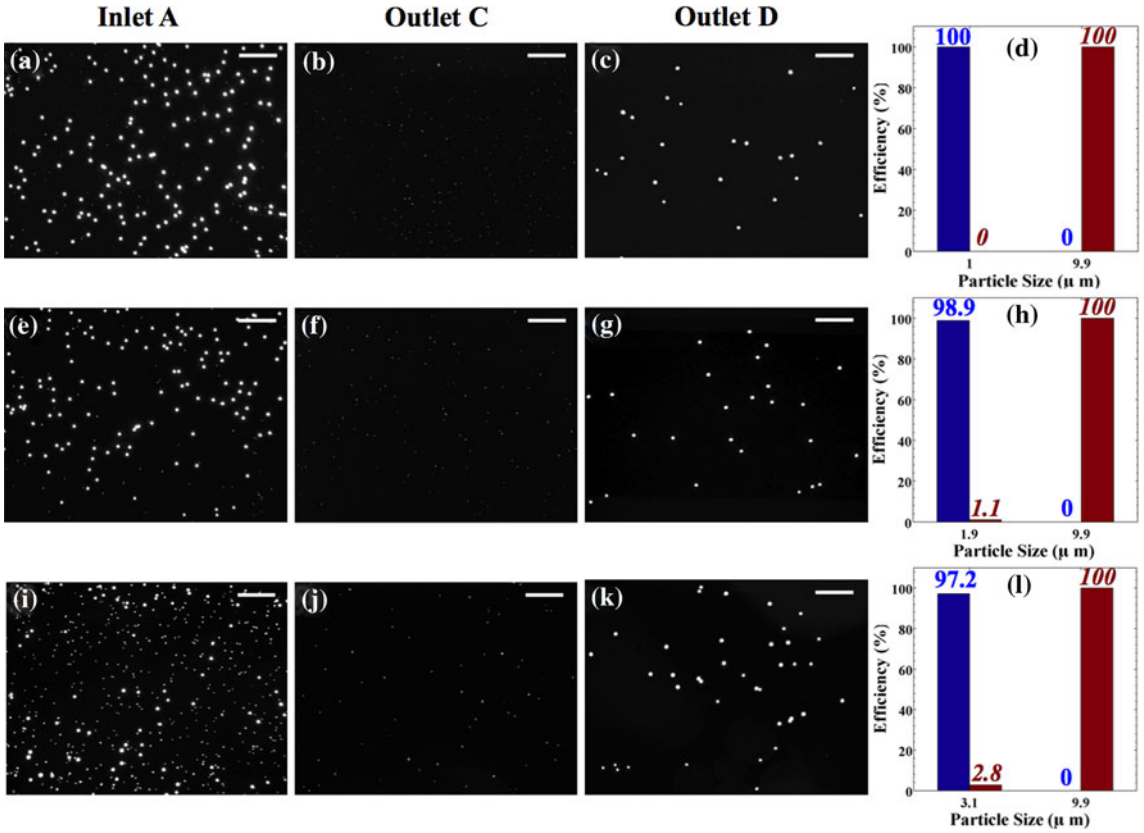

Fig. 3 Representative fluorescent images of particles mixture collected before separation (at Inlet *A*) and after separation (at Outlets *C* and *D*), and the particles remaining and separation efficiencies, **a–d** were for 1 and 9.9 μm particles mixture; **e–h** were for 1.9 and 9.9 μm particles mixture; **i–l** were for 3.1 and 9.9 μm particles mixture. *Blue bar* (with normal number on top) indicates the remaining efficiency, while the *red bar* (with Italic number on top) indicates the separation efficiency of particles after passing through the separation region. The *scale bars* represent 300 μm

close to the sidewall of the channel and exited the device through Outlet C (see Fig. 3b, particle sample collected from Outlet C after magnetic field application), and virtually all large particles were observed to migrate into Outlet D (see Fig. 3c, particle sample collected from Outlet D after magnetic field application). The remaining and separation efficiencies for both particles are shown in Fig. 3d. 100% of small particles exited through Outlet C, and 100% of large particles migrated into Outlet D. Figure 3e–h and i–l depicts the images and efficiencies for 1.9 μm/9.9 μm mixture separation and 3.1 μm/9.9 μm mixture separation, respectively. The separation efficiencies of large particles for both mixtures were 100%, while the remaining efficiencies of small particles were 98.9% for 1.9 μm particles and 97.2% for 3.1 μm particles. As the difference between particle sizes becomes smaller, the difference in the magnitude of the magnetic buoyancy forces on the particles will decrease accordingly, which leads to smaller difference in the spatial separation.

Compared to the existing ferrofluid based (Kose et al. 2009; Yellen et al. 2005) or magnetic aqueous solution based (Winkleman et al. 2007) particle separation technique, our approach offers the following advantages: (i) the particle separation throughout ($\sim 10^5$ particles/h) is high, and it is possible to increase the throughput further by increasing the flow rates and magnetic fields; (ii) the separation efficiency of our approach is comparable or higher than the efficiencies of existing techniques; (iii) the device fabrication is low cost and does not require microfabricated electrodes or micromagnets; (iv) the separation system is simple and only requires the microfluidic device and a stack of permanent magnets. Some of the limitations of this approach include: (i) ferrofluids are opaque, thus making the particle motion recording and sample analysis difficult, (ii) high flow rates within the device may have a negative effect on the biological entities such as cells if this approach is adopted for biological applications.

5 Conclusions

We have developed a new size-based microparticle separation approach using ferrofluids. We have shown label-free binary particles separation in a continuous flow microfluidic device with high throughput and efficiency. The results presented here demonstrate the potential of continuous separation of non-magnetic object inside ferrofluids within microfluidic devices. Separation of particles is also possible through existing techniques such as dielectrophoresis, optical force, and magnetic bead labeling methods. However, our approach offers low cost, high throughput and high efficiency simultaneously in a label-free manner.

Acknowledgments We thank Gareth Sheppard for his help on making the masks. This research was financially supported by the Office of the Vice President for Research at the University of Georgia.

References

Ganatos P, Pfeffer R, Weinbaum S (1980) A strong interaction theory for the creeping motion of a sphere between plane parallel boundaries 2. Parallel motion. J Fluid Mech 99:755–783

Gerber R, Takayasu M, Friedlaender F (1983) Generalization of HGMS theory: the capture of ultra-fine particles. IEEE Trans Magn 19(5):2115–2117

Huang LR, Cox EC, Austin RH, Sturm JC (2004) Continuous particle separation through deterministic lateral displacement. Science 304(5673):987–990

Kose AR, Fischer B, Mao L, Koser H (2009) Label-free cellular manipulation and sorting via biocompatible ferrofluids. Proc Natl Acad Sci USA 106:21478–21483

Krishnan GP, Leighton DT (1995) Inertial lift on a moving sphere in contact with a plane wall in a shear-flow. Phys Fluids 7(11):2538–2545

MacDonald MP, Spalding GC, Dholakia K (2003) Microfluidic sorting in an optical lattice. Nature 426(6965):421–424

Mao L, Koser H (2005) Ferrohydrodynamic pumping in spatially traveling sinusoidally time-varying magnetic fields. J Magn Magn Mater 289:199–202

Mao L, Koser H (2006) Towards ferrofluidics for micro-TAS and lab on-a-chip applications. Nanotechnology 17(4):S34–S47

Nolan JP, Sklar LA (1998) The emergence of flow cytometry for sensitive, real-time measurements of molecular interactions. Nat Biotechnol 16(7):633–638

Rinaldi C, Zahn M (2002) Effects of spin viscosity on ferrofluid flow profiles in alternating and rotating magnetic fields. Phys Fluids 14(8):2847–2870

Rosensweig RE (1966) Fluidmagnetic buoyancy. AIAA J 4:1751–1758

Rosensweig RE (1985) Ferrohydrodynamics. Cambridge University Press, New York

Rosensweig RE, Lee WK, Siegell JH (1987) Magnetically stabilized fluidized-beds for solids separation by density. Sep Sci Technol 22(1):25–45

Skjeltorp AT (1983) One- and two-dimensional crystallization of magnetic holes. Phys Rev Lett 51(25):2306–2309

Staben ME, Zinchenko AZ, Davis RH (2003) Motion of a particle between two parallel plane walls in low-Reynolds-number Poiseuille flow. Phys Fluids 15(6):1711–1733

Takagi J, Yamada M, Yasuda M, Seki M (2005) Continuous particle separation in a microchannel having asymmetrically arranged multiple branches. Lab Chip 5(7):778–784

Toner M, Irimia D (2005) Blood-on-a-chip. Annu Rev Biomed Eng 7:77–103

Voldman J (2006) Electrical forces for microscale cell manipulation. Annu Rev Biomed Eng 8:425–454

Winkleman A, Perez-Castillejos R, Gudiksen KL, Phillips ST, Prentiss M, Whitesides GM (2007) Density-based diamagnetic separation: devices for detecting binding events and for collecting unlabeled diamagnetic particles in paramagnetic solutions. Anal Chem 79(17):6542–6550

Xia Y, Whitesides GM (1998) Soft lithography. Annu Rev Mater Sci 28(1):153–184

Yamada M, Seki M (2005) Hydrodynamic filtration for on-chip particle concentration and classification utilizing microfluidics. Lab Chip 5(11):1233–1239

Yellen BB, Hovorka O, Friedman G (2005) Arranging matter by magnetic nanoparticle assemblers. Proc Natl Acad Sci USA 102(25):8860–8864

Yung CW, Fiering J, Mueller AJ, Ingber DE (2009) Micromagnetic-microfluidic blood cleansing device. Lab Chip 9(9):1171–1177

Zahn M, Greer DR (1995) Ferrohydrodynamic pumping in spatially uniform sinusoidally time-varying magnetic fields. J Magn Magn Mater 149(1–2):165–173